FERMILAB-Conf-04/005-E January 2004

HADRON CALORIMETERS FOR FUTURE HADRON COLLIDERS

JIM FREEMAN

Fermi National Accelerator Laboratory, Batavia, IL 60510, USA
E-mail: freeman@fnal.gov

Hadron calorimeters are essential for jet and neutrino physics at collider experiments. Current hadron calorimeters for the ATLAS and CMS detectors are described. Increased energy and luminosity of future hadron colliders place constraints on detector technology. Difficulties for operation of the current detectors in future hadron collider environments are discussed. New experiments for future colliders should take notice of physics processes during jet evolution that place fundamental limits on performance of the calorimeter to reconstruct jets. A technique of incorporating tracking information to improve jet resolution is described. Future detectors should be designed with these constraints in mind. Possible avenues of exploration for future technology are described.

1. Introduction

Hadron calorimeters take part in reconstructing energy of hadrons in jets and underlying events. Important performance issues include: eta/phi segmentation suitable for jet clustering; depth segmentation and longitudinal thickness to contain the hadron shower and tag possible leakage; energy resolution sufficient not to degrade jet energy resolution; hermetic eta/phi coverage to minimize false missing E_T; and time resolution sufficient to correctly identify the beam crossing that the energy deposition comes from.

The Large Hadron Collider (LHC) at CERN is the next generation of hadron colliders. It will collide 7 GeV protons against 7 GeV protons and start operation in 2007. Its design luminosity is 10^{34} cm^2/sec. Two large general purpose detectors are being constructed to operate at the LHC. They are ATLAS and CMS.

The ATLAS calorimeter is based on two technologies. Liquid Argon (LAr) calorimeters are used for the electromagnetic compartment in the central region and for both electromagnetic and hadronic calorimetry in the high eta region, $\eta < 3.2 < 4.5$ [1]. In the central region of ATLAS, scintillator tile/fiber calorimeters are employed to measure hadrons[2].

The forward ATLAS LAr calorimeter uses a novel design with electrode tubes rather that the usual parallel gaps. The cylindrical gap defined by the outer tube and inner solid rod ranges from 250 to 500 microns. This geometry allows for very fast drift times for the ionization and reduces the problem of space charge formation at very high rates.

The ATLAS outer hadron calorimeter in the central region is made from iron plates/scintillating tiles/wavelength-shifting fiber readout. Instead of the more standard arrangement of scintillator tile samples in planes of $\sim$ constant R, in this calorimeter the plates are arranged in planes of $\sim$ constant Z. Wavelength shifting fibers run parallel to the edges of the tiles in the R direction and carry the light to photomultipliers at the outer radius.

The CMS calorimetry is also based on multiple technologies. In the central region, $\eta < 3$, the electromagnetic calorimeter is composed of $PbW0_4$ crystals. Behind that is the hadron calorimeter based on scintillator tile/fiber. In the forward region, $\eta > 3$, quartz fiber Cerenkov calorimetry is employed.

The central hadron calorimeters of CMS use scintillator tiles with wavelength shifting fibers sandwiched between layers of brass absorber [3]. The fibers are read out into HPDs. The tiles form projective towers and fibers from each tile in longitudinal depth is ganged together optically at the input of the HPD.

The forward calorimeter for CMS is a new design: Quartz fibers placed in an iron matrix. The quartz fibers capture Cerenkov light produced by shower secondaries. Fibers are bundled into towers and the light is carried to photomultiplier tubes. The light yield is roughly 1 photoelectron per 2 GeV of energy deposition.

2. Issues for the SLHC

The Super LHC (SLHC) is an upgrade program for the LHC [4]. Initially the upgrade will increase the instantaneous luminosity by a factor of 10 and is contemplated for 2013. The upgrade will be achieved by increasing the luminosity per bunch by a factor of 5, and increasing the number of bunches by a factor of 2. The initial 25ns beam-crossing period of the LHC will thus be reduced to 12.5ns. A longer term upgrade of beam energy is also contemplated, which if implemented, would increase the beam energy from 7 to 14 GeV.

Table 1 describes the parameters for the LHC, SLHC, and VLHC colliders.

Table 1. Characteristics for the LHC, SLHC, and VLHC. Assumptions made are that trackers and calorimeters can always identify the correct bunch crossing. For the VLHC, the total inelastic cross section is taken at 130 mB, charged multiplicity is $dN/d\eta = 10$, and $< E_T >$ per particle is 1 GeV.

	LHC	SLHC	VLHC
$\sqrt{s}$	14 TeV	14 TeV	100 TeV
L	10^{34}	10^{35}	10^{34}
$\int Ldt$	100 fb^{-1}/yr	1000 fb^{-1}/yr	100 fb^{-1}/yr
Bunch Spacing dt	25ns	12.5ns	19ns
Nr interactions per x-ing	20	100	25
$dN_{ch}/d\eta$ per x-ing	100	500	250
Relative tracker occupancy	1	5	2.5
Relative pile-up noise	1	2.2	2.5
Dose central region	1	10	5

These upgrades put new demands on the calorimeters. Since these new demands were not foreseen at the time of the initial design, we need to consider their impact on the detectors and possible required upgrades.

Four principle effects of the SLHC environment are radiation damage; radio-activation of the detector; instantaneous rate effects; and bunch determination. As shown in Table 1, radiation levels increase by a factor of 10 in the SLHC era. Figure 1 shows the dose per year of SLHC operation in the CMS calorimeters vs. the detector η [5]. Curves for the electromagnetic and hadronic calorimeters are shown. The curve for the electromagnetic calorimeter stops at $\eta = 3$, the edge of the electromagnetic detector. The hadron curve continues to $\eta = 5$, the high η boundary of the forward Cerenkov calorimeter. The radiation expected for the hadron calorimeter varies from about 1 Mrad/year at eta=2 to 6 Mrad/year at $\eta = 3$. Note that for $\eta > 3$, the calorimeter is based on quartz fiber, a very radiation resistent material.

Figure 2 shows the effect of radiation on tile/fiber of the type employed in CMS hadron calorimeters [6]. We see an exponential decrease in light output with exposure to radiation. A practical limit of operation is 5 Mrad, where the light yield has decreased by a factor of 3 from it's initial value. This implies that during SLHC operation the scintillators at eta=3 would have to be replaced annually. This is not feasible.

Activation of the calorimeter detectors is an important issue at the SLHC. After 1 year of running at the SLHC at design luminosity and with one day of cool-down, activities of $1-3*10^3$ μsieverts/hr are present on the

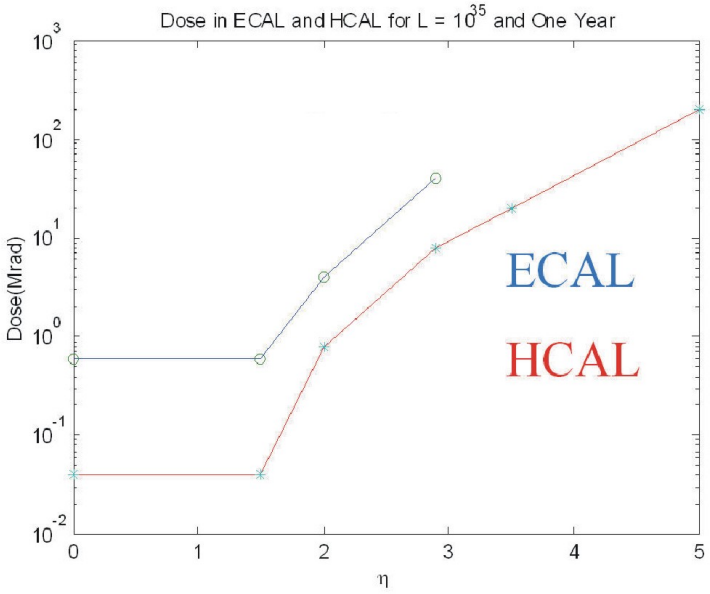

Figure 1. Radiation dose per year at the SLHC design luminosity of 10^{35}.

front face of the CMS HF, and $1-3*10^2$ μsieverts/hr on the front face of the HE [7]. A practical exposure limit for radiation workers is 50 μsieverts/hr. We see that high eta regions for the endcap hadron calorimeter and all of the face of the forward hadron calorimeter exceed those limits. From this we realize that any upgrades to these regions need to be robust enough to survive the full period of the SLHC operation. (10 years at 10^{35} luminosity). Currently there are no developed technologies that can work in the CMS HCAL endcap environment for this extended period. In the section on R&D some ideas for development will be discussed.

Liquid argon calorimeters do not suffer radiation damage like the scintillator ones do. However they have problems at very high ionization deposition rates. As more and more energy is deposited per second, and more and more ionization is formed in the LAr, at some point space charge effects become important. These space charge effects can distort and eventually overwhelm the applied electric field. This point it know as the critical ionization density. It is dependent on the ion mobility of the liquid, the applied high voltage, and the gap width.

The dependence proportional to

$$\frac{V^2}{d^4\mu}$$

with V the high voltage applied across the gap, d the gap width, and μ the mobility.

Table 2 show the critical ionization density as well as the anticipated ionization densities as a function of eta for 10^{34} and 10^{35} operation [1]. From table 2 we see that the ATLAS liquid argon system will stop operating at $\eta = 1.5$. We note that the FCAL, based on tube electrodes with very small gaps, is immune to this problem. Therefore the Endcap ATLAS liquid Argon system will need to be modified. Suggested possibilities include operating this region with pressurized noble gas which will have a much higher ion mobility.

In the SLHC environment the bunches will cross with a 12.5ns period, twice as fast as initial LHC operation. It is important to correctly identify the bunch crossing that energy deposition in the calorimeter is due to. In this way the entire event (calorimeters, tracking, muon system) can be put

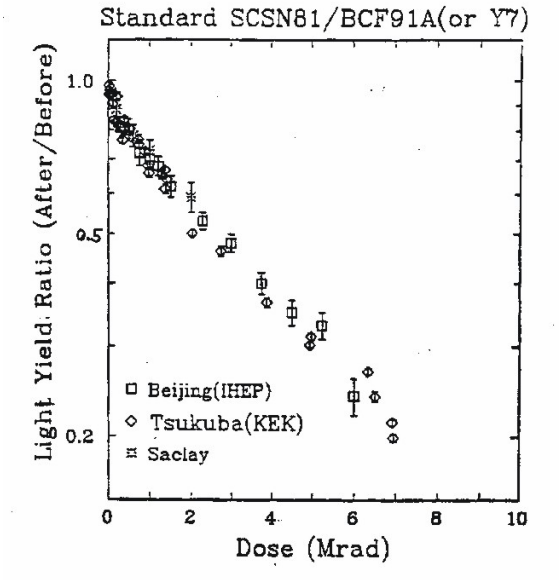

Figure 2. Radiation damage for scintillator tile/fiber configuration.

Table 2. Critical ionization density for the ATLAS liquid argon calorimeters and expected ionization for the LHC and the SLHC.

	Critical Density	Atlas 10^{34}	Atlas 10^{35}
Barrel EM, $\eta = 0$	$5 * 10^6$	$0.5 * 10^5$	$5 * 10^5$
Barrel EM, $\eta = 1.3$	$4 * 10^6$	$1.2 * 10^5$	$1.2 * 10^6$
Endcap EM, $\eta = 1.4$	$3 * 10^6$	$1.3 * 10^5$	$1.3 * 10^6$
Endcap EM, $\eta = 3.2$	$5 * 10^6$	$2.5 * 10^6$	$25 * 10^6$
FCAL, $\eta = 3.2$	$1500 * 10^6$	$2.5 * 10^6$	$25 * 10^6$
FCAL, $\eta = 4.5$	$1500 * 10^6$	$130 * 10^6$	$1300 * 10^6$

together for analysis.

The CMS HF calorimeter uses Cerenkov light for energy measurement. This is a very fast signal. Figure 3 shows a testbeam measurement of the Cerenkov pulse shape coming from the calorimeter. We see that the full width/half max is about 15ns. There will be no problem associating the energy to a 12.5 ns bucket. The scintillator signal on the other hand is significantly slower.

Figure 4 shows the measured signal from the HE calorimeter. We see a fast rise and a slower exponential fall due to the decay time of the wavelength shifting flor. The analog signal is digitized in a 40 Mhz flash ADC.

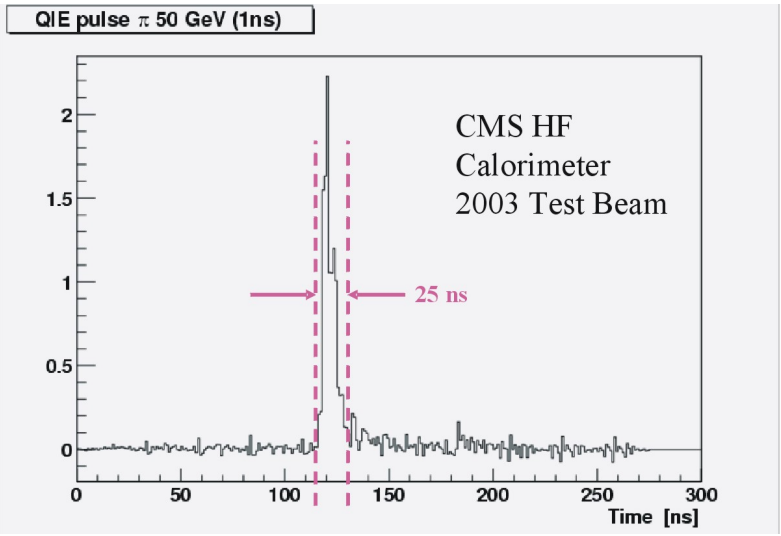

Figure 3. Average pulse shape for CMS HF Calorimeter as measured in 2003 testbeam.

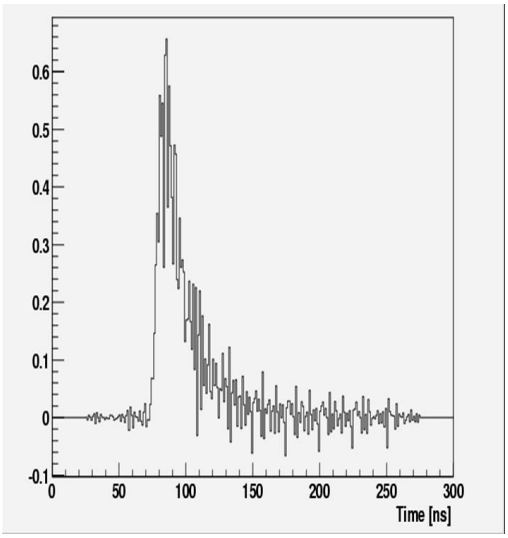

Figure 4. Average pulse shape for CMS HE Calorimeter as measured in 2003 testbeam.

Figure 5 shows the digitized signal for different relative phases of the time between the 40 Mhz clock edge and the particle arrival time as seen in the testbeam. (Note that in testbeam environment the beam is basically continuous and has no correlation to the arbitrary phase of the electronics clock. However we can and do measure the time difference between the clock edge and the beam trigger. We can then bin the events in bins of measured phase difference). In this figure each histogram contains events of the same relative phase. Each histogram differs from its neighbor by 1ns of phase. The histogram shows the average pulse shape for the events where each bin is one 40 Mhz clock cycle. From this figure we see that the average event shape changes as a function of the phase. The average shape for events differing by 12 ns (12 histograms) is distinctly different. Therefore we can form a variable based on event shape that will give us information on the actual event time.

In Fig 6 we plot on the vertical scale the energy weighted mean time of events based on the flash ADC data. On the horizontal axis we plot the corresponding true measured time from the testbeam trigger. We see a very strong correlation, with an rms of a few nanoseconds. From this we conclude that we can accurately determine the bunch crossing for energy deposited in the calorimeter, even operating at 80Mhz. Monte Carlo studies

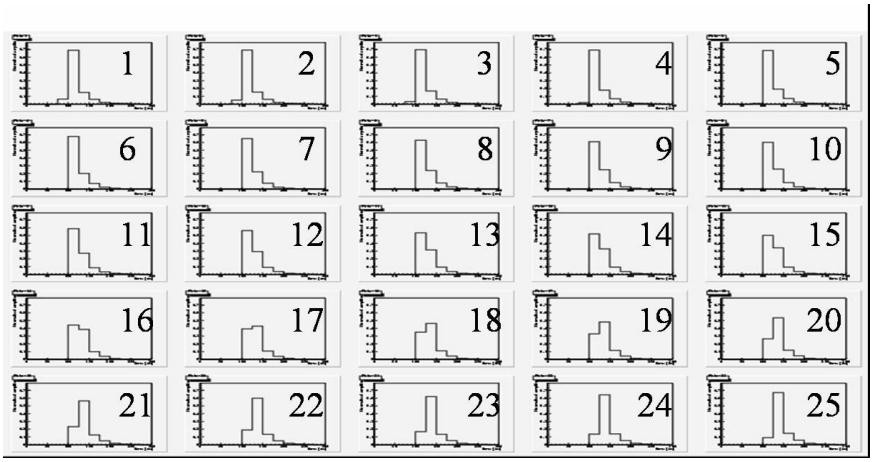

Figure 5. Average digitized pulse shape for constant relative phases for CMS HE Calorimeter as measured in 2003 testbeam. Each histogram is average shape for events with a unique phase of the clock relative to the beam trigger timing. Each bin is 25 ns wide. Upper left histogram corresponds to phase = 1ns and lower right to phase = 25ns. Note that the average pulse shape repeats after 25ns.

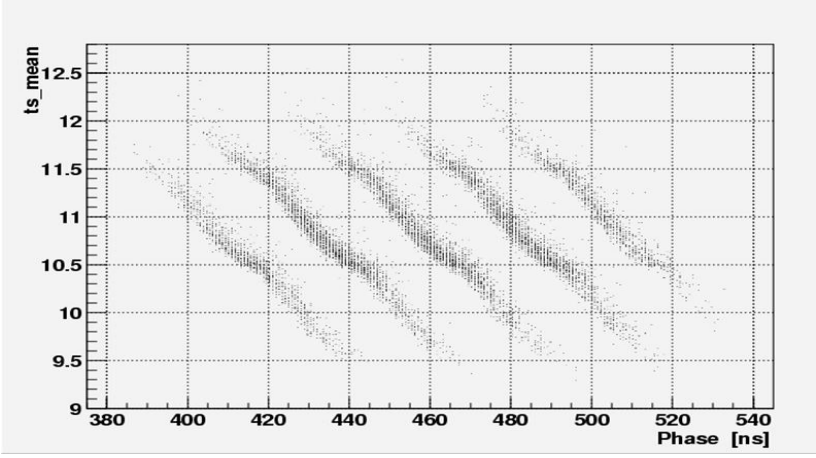

Figure 6. Scatter plot of event time fitted using event shape(vertical) vs. event time measured using beamline counters.

of this effect, based on testbeam data, show that correct bunch ID can be made to energy depositions as low as 1 GeV.

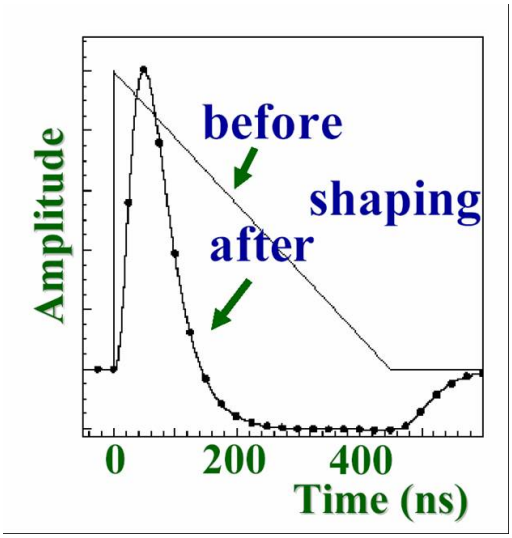

Figure 7. Pulse shape for ATLAS LAr calorimeter before and after pulse-shaping.

Liquid Argon Calorimetry is even slower than scintillator based calorimetry. Figure 7 shows the response from the ATLAS LAr calorimeter before and after shaping [8]. We note that after shaping, the signal looks very much the same as that for the CMS scintillator, Fig 4. Based on this we can conclude that the ATLAS calorimeter should also be able to form correct bunch ID. The D0 LAr calorimeter at Fermilab can also use event shape to make a timing estimation. Their measured resolution is 4ns/E with E in GeV.

3. Energy Flow

Jet and single particle energy resolution can be improved by use of tracking information when available. Figure 8 shows energy resolution vs. energy for generic "good" electromagnetic (dashes) and hadronic (dots) calorimeter and for a tracking system performing like the CMS tracker [9]. We note that for low energies (less than ∼100-200 GeV) the tracking information is more accurate than the calorimeter. Thus if we can use the tracking information for these particles we can get an improved measurement. This idea is known as "energy flow" and has been used for jet resolution improvement by CDF [10]. When an "isolated" energy deposition in the calorimeter can be associated with a charged track, and if the tracking measurement is more

accurate than the calorimeter measurement, use the tracking measurement, and subtract out the associated energy in the calorimeter. This technique can be used both for jet clustering and for global studies like missing Et. Figure 9 shows CDF results on photon+jet momentum balancing for the cases with and without energy flow. A 24% improvement in jet energy resolution is seen. Monte Carlo studies for CMS have achieved similar results. To take full advantage of this technique, the energy depositions in the calorimeter should be uniquely associated with the charged track. This argues for "small" transverse towers in the calorimeter, where small is determined by the lateral shower development, the moliere radius or the interaction length.

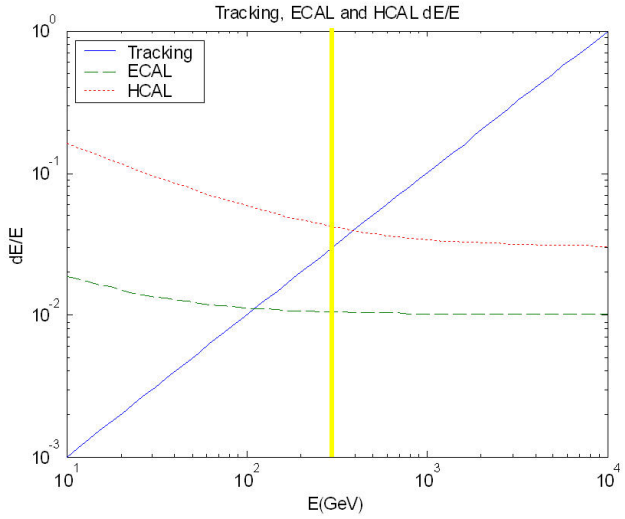

Figure 8. Single particle resolution dE/E vertical scale vs energy. Cases of Tracker measurement dPt/Pt**2 $= 10^{-4}$, Ecal $10\%/\sqrt{E}$, and HCAL $50\%/\sqrt{(}E$ are shown. Note that for particles of energy less than about ∼200 GeV, the tracker makes a more accurate measurement than the calorimeters.

4. Requirements for a New Detector

Both the ATLAS and CMS calorimeters exist, and modifications for operation in the SLHC will not require their replacement. However it is interesting to contemplate design of new calorimeters for a future super

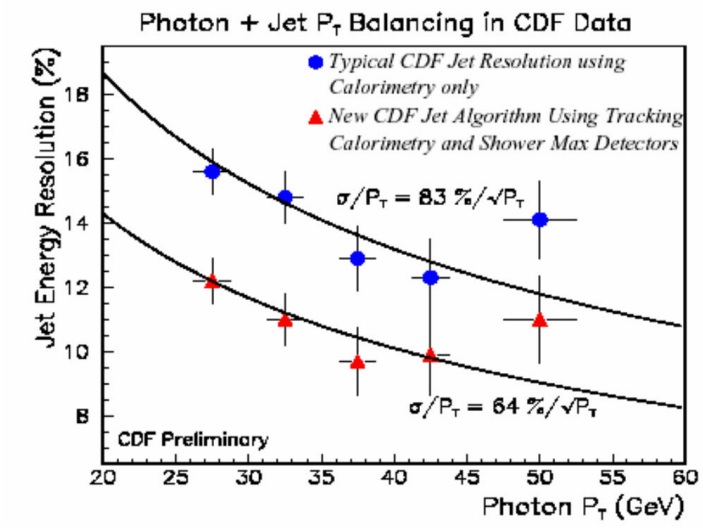

Figure 9. Jet resolution vs. photon energy for jet+gamma events. The improvement in jet resolution using energy flow is shown.

collider, the VLHC for example. In this section we will review some of the important considerations for a new calorimeter design.

We have just seen that the "energy flow" technique promises to make substantial improvement to the jet energy measurement. Therefore we should design the new calorimeter to take advantage of it. Figure 10 shows the transverse shower energy density as a function of radius from the shower core in an iron calorimeter [11,12]. we see a very fast falloff at small R. A transverse tower size of 5cm looks like a reasonable choice. Tower sizes larger than that will start to lose position information.

Figure 11 shows longitudinal shower development for 6 separate showers in a test calorimeter[13]. This test calorimeter had 96 longitudinal readout segments, each 0.1 interaction lengths thick. It is clear that there are very large fluctuations in the energy deposition of the different showers. Therefore fine longitudinal segmentation of the hadron calorimeter does not make sense. It will simply be measuring the random fluctuations in the shower development.

Figure 12 shows the ratio of shower leakage divided by energy lost by neutrinos as a function of depth of the calorimeter [14]. The simulated events are 10 TeV jets. We see that at about 10-12 lambda of calorimeter

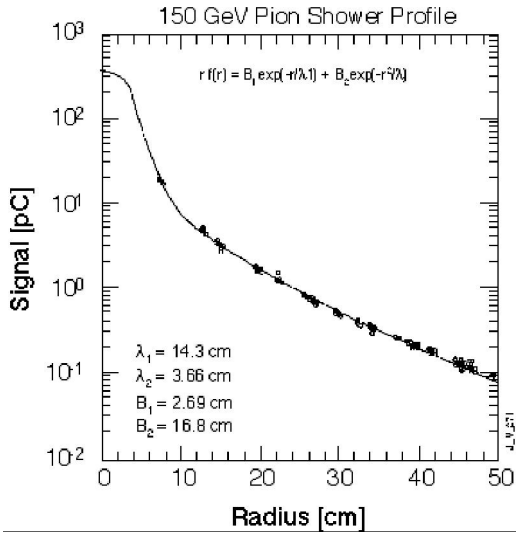

Figure 10. Shower energy density vs. radial distance from the shower core.

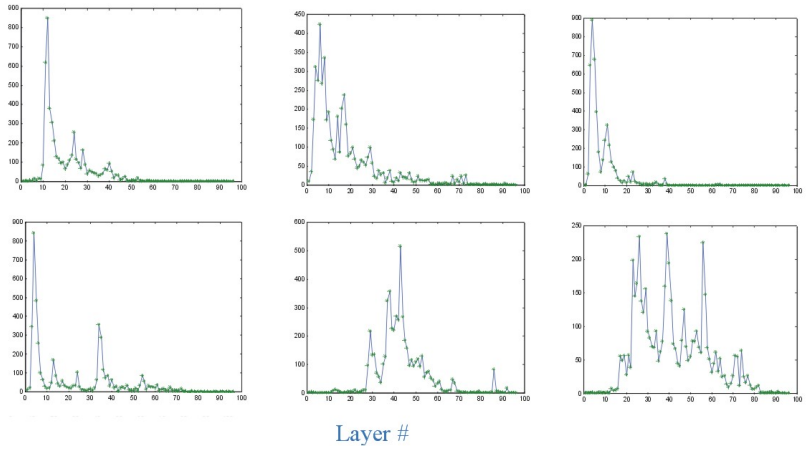

Figure 11. Longitudinal profiles for six 100 GeV Pions. 96 layers of independent readout.

thickness the neutrino losses dominate. Thus the natural thickness of a hadron calorimeter is about 12 lambda.

Energy resolutions of the calorimeters should be chosen so that they do

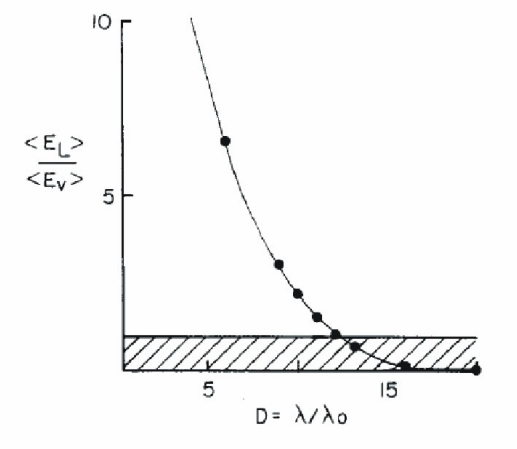

Figure 12. Ratio of energy loss due to longitudinal leakage divided by loss due to neutrinos vs. longitudinal thickness of calorimeter in interaction lengths.

not contribute substantially to jet energy resolution. It turns out that jet energy resolution is not dominated by detector effects but rather by intrinsic physics of jet evolution[15]. Figure 13 shows fractional mass resolution for $Z \rightarrow jet + jet$ in the CMS detector. The 4 histograms show: a) parton level; b) including initial state radiation effects (ISR); c) b + final state radiation (FSR); and d) including additionally fragmentation effects. In all 4 histograms, no detector effects are simulated. Figure 14 models a "CMS-like" detector with a calorimeter resolution of $120\%/\sqrt{E}$. In histogram a) there is fragmentation but no initial or final state radiation; b) adds both ISR and FSR ; and c) models a calorimeter with $60\%/\sqrt{E}$. We conclude from this that the single most important effect in di-jet mass resolution is final state radiation. Energy is carried away from the system by the radiation. We conclude that calorimeter energy resolution has very little (or no) effect on di-jet mass resolution.

The case in the linear collider environment may or may not be different. If jets due to FSR can be correctly associated with the parton that radiated, it may be possible to alleviate some of the resolution degradation due to FSR. If sufficiently accurate event reconstruction can be done in the LC environment (with in-principle cleaner underlying events) then the effect of calorimeter energy resolution may begin to be seen.

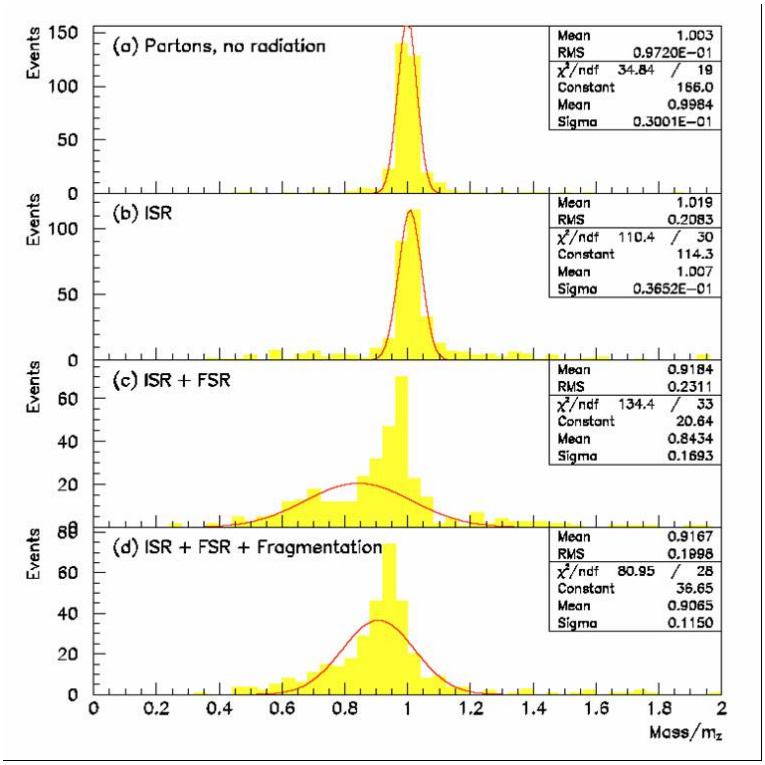

Figure 13. CMS Z to 2 jet decays. Fractional mass resolution for: a) parton level; b) and initial state radiation; c) and final state radiation; d) and fragmentation. No detector effects are simulated.

5. New Directions

The operating environment at future hadron colliders emphasizes hadron calorimeters that are radiation hard, fast, and able to be segmented to take advantage of energy flow. Cerenkov calorimeters have the potential for being very fast and radiation hard. A natural extension of current technology would be implementing quartz fiber calorimetry in more central regions of a new detector. Another possibility may be a quartz plate calorimeter with wavelength shifting fiber readout. Challenges in this approach are to develop appropriate radiation hard wavelength shifting materials. Total light yield is another potential problem. High pressure gas can also be used as the Cerenkov medium, as described in reference [16].

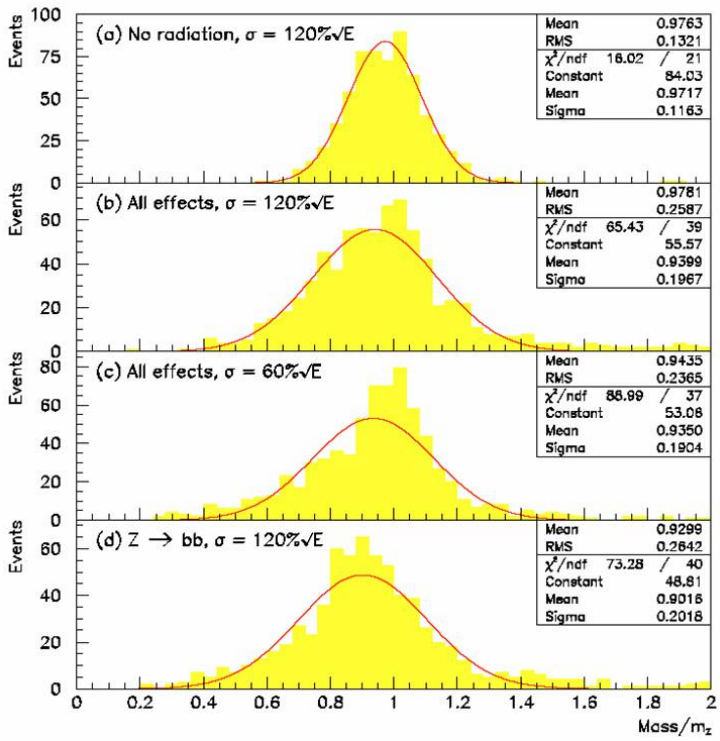

Figure 14. CMS Z to 2 jet decays. CMS detector effects are simulated. Fractional mass resolution for: a) calorimeter resolution = $120\%/\sqrt{E}$, no radiation; b) all radiation and fragmentation, $120\%/\sqrt{E}$; c) all radiation and fragmentation, calorimeter resolution = $60\%/\sqrt{E}$; d) all effects for Z to $b-\bar{b}$.

6. Conclusions

We have seen that the experimental environment in future colliders will challenge the operation of hadron calorimeters. The SLHC upgrade will increase the luminosity by a factor of 10. This increase will negatively affect the endcap regions of both ATLAS and CMS. For the case of ATLAS, the specific ionization will cause charge loss. This can be circumvented by a change of the ionization medium, perhaps to noble gas. For the case of CMS, the increased radiation damage to the scintillators in the endcap region will make them inoperative. A new calorimeter technology is needed here.

For new colliders farther in the future, new calorimeters will need to

be designed. New calorimeters should be designed with the concept of "energy flow" held in mind. This method of jet clustering has the potential to improve the jet resolution by up to 20%. Reasonably small transverse tower size is important to this technique. We have seen that calorimetric energy resolution is not important to the jet resolution, dominated by final state resolution.

There are several new technologies that may hold promise to calorimeters in future colliders. Among these are Cerenkov calorimeters made from quartz plate with inorganic wavelength-shifting fibers to carry light out, and gas Cerenkov calorimeters.

Acknowledgments

I would like to thank Dan Green, Jim Rohlf, and Weimin Wu for valuable discussions during the preparation of this paper. I would also like to acknowledge Shuichi Kunori and Jordan Damgov for their work in analysis of CMS HCAL 2003 testbeam data that is presented here.

References

1. ATLAS Liquid Argon Calorimeter TDR, CERN/LHCC 96-41.
2. ATLAS Tile Calorimeter TDR, CERN/LHCC 96-42.
3. CMS Hadron Calorimeter TDR, CERN/LHCC 97-31.
4. Physics Potential and Experimental Challanges of the LHC Upgrade, CERN-TH/2002-078.
5. M. Huhtenin, private communication.
6. Radiation Damage and Performance of Scintillator-fiber System in Calorimetry, V. Hagopian et al., 4th International Conference on Calorimetry in High-energy Physics, La Biodola, Italy, 19-25 Sep 1993.
7. M. Huhtenin, these proceedings.
8. The Readout System for ATLAS Liquid Argon Calorimeters, I. Riu, Proc. 8^{th} Workshop on Electronics for LHC Experiments, Colmar, France, Sept. 2002.
9. Energy Flow in CMS Calorimetry, D. Green, Fermilab-FN-0709.
10. Physics at Run II, Fermilab-Pub-00/349, 469-470.
11. Hadronic and Electromagnetic Tranverse Calorimetric Segmentation, W. Wu, et al., Fermilab-FN-589.
12. F. Binon, et al., Nucl. Instrum. Methods 206 373(1983).
13. Beam Tests of Composite Calorimeter Configurations from a Reconfigurable-stack Calorimeter, A. Beretvas et al., NIM A329(1993), 50-61.
14. Depth Requirements in SSC Calorimeters, D. Green, et al., Fermilab-FN-570.
15. Dijet Mass Resolution of the CMS Calorimeter, D. Green et al., CMS Note 1998/026.
16. Explicitly Radiation Hard Fast Luminosity Monitor, E. Torrence et al., Arlington Linear Collider Workshop, Jan. 2003.